Periodic Orbits of Nonlinear Relative Dynamics and Satellite Formation

Bando, Mai
Research Institute for Sustainable Humanosphere, Kyoto University

Ichikawa, Akira
Department of Aeronautics and Astronautics, Graduate School of Engineering, Kyoto University : Professor

出版情報：Journal of Guidance, Control, and Dynamics. 32 (4), pp.1200-1208, 2009-07-01.
American Institute of Aeronautics and Astronautics
バージョン：
権利関係：

Periodic Orbits of Nonlinear Relative Dynamics and Satellite Formation

Mai Bando *

Kyoto University, Gokasho, Uji, Kyoto 611-0011, Japan

and

Akira Ichikawa †

Kyoto University, Kyoto 606-8501, Japan

ABSTRACT

In this paper, leader-follower formation and reconfiguration problems based on the periodic orbits of the nonlinear relative dynamics along a circular orbit are considered. First, initial conditions of coplanar and non-coplanar relative orbits are characterized by the initial true anomaly, mean motion, semimajor axis, eccentricity and inclination angle of the follower's inertial orbit. Based on the property of null controllability with vanishing energy of the Hill-Clohessy-Wiltshire equations, L_1 suboptimal feedback controllers are designed via the linear quadratic regulator theory. Simulation results for three examples are given. A comparison with the reconfiguration problem based on the periodic orbits of the Hill-Clohessy-Wiltshire equations shows that replacement by nonlinear periodic orbits does not increase the L_1-norm of the feedback control.

1 Introduction

The relative motion of one satellite with respect to another in a circular orbit is described by autonomous nonlinear differential equations. The linearized equations around the null solution were introduced by Clohessy and Wiltshire [1] to analyze satellite rendezvous, and are now known as Hill-Clohessy-Wiltshire (HCW) equations [2–4]. Since then, the HCW equations were used by many authors to study rendezvous problems (see [5] and references therein). Typical problems involve fixed-time and fixed-end conditions, impulsive maneuvers, the total velocity change as a cost function, and optimal solutions are sought. Prussing [6, 7] derived two-, three- and four-impulse solutions. Carter [8] and Carter and Brient [5, 9] obtained necessary and sufficient conditions for optimal solutions for both HCW equations and Tschauner-Hempel

*Mission Research Fellow, Research Institute for Sustainable Humanosphere, m-bando@rish.kyoto-u.ac.jp

†Professor, Department of Aeronautics and Astronautics, Graduate School of Engineering, ichikawa@kuaero.kyoto-u.ac.jp.

(TH) equations, which are linearized equations of the relative motion along an eccentric orbit. A general but succinct formulation of rendezvous problems is given in [5] and optimal solutions are derived in an elementary manner. Jezewski and Donaldson [10] considered a free-time problem, and obtained two-impulse solutions. The Space Shuttle project in 1980's and expected future space missions lead to a new concept of formation flying, and the HCW equations were used by many researchers to study formation problems. In formation flying, the satellite in the circular reference orbit is often referred to as a leader, and the other as a follower. In earlier days, formationkeeping problems, where the final desired state is the origin, were studied. Vassar and Sherwood [11] assumed impulse maneuvers at given sampling times, and employed the discrete-time linear quadratic regulator (LQR) theory. Leonard, Hollister and Bergmann [12] used three-valued differential drag between two satellites for controlling the relative motion. Redding, Adams, and Kubiak [13] proposed a controller based on feed-forward control and the discrete-time LQR theory. Motivated by new developments in propulsion technologies, Kapila, Sparks, and Buffington [14] employed pulse control, and designed stabilizing feedback controls by the discrete-time LQR theory.

The HCW equations possess periodic solutions, which are useful as temporary orbits before mission, and for proximity operations such as inspection and repair. They are also used for satellite formation. Kang, Sparks, and Banda [15] used feedback linearization and the continuous-time LQR theory to track a periodic solution of the HCW equations. Campbell [16] considered a reconfiguration problem between two periodic solutions, and formulated the minimum-time problem, and a minimum-fuel problem, where the time interval is finite and the cost function is the absolute integral of the thrust. Schaub [17] derived the description of the relative orbit in terms of orbit element differences for both circular and eccentric reference orbits. Vaddi et. al. [18] considered formation and reconfiguration problems using orbit element differences, and obtained a two-impulse solution. Palmer [19] considered a finite-time formation problem, where the square integral of the thrust accelerations is minimized, and analytic solutions for the thrust functions are given. Periodic solutions of the TH equations, which give relative orbits along an eccentric reference orbit, were characterized by Inalhan, Tillderson and How [20], and the initialization procedure to periodic motion was given.

It is well-known in the LQR theory that a large penalty on control results in smaller inputs [15]. For a certain class of linear systems, the L_2-norm of the feedback control given by the LQR theory tends to zero as the penalty on control becomes infinitely large. This property is referred to as null controllability with vanishing energy (NCVE), and was introduced for infinite dimensional systems by Priola and Zabczyk [21] together with necessary and sufficient conditions. A more precise definition is given as follows. A linear system is null controllable with vanishing energy (also denoted by NCVE) if any state can be steered to the origin by a control with an arbitrarily small L_2-norm, as the control duration becomes arbitrarily large. Recently, it was remarked by Shibata and Ichikawa [22] that the HCW system with three independent thrusters is NCVE. This property assures the design of a feedback controller with an arbitrary small L_2-norm through the LQR theory taking a small (large) penalty matrix on state (control, respectively). Using periodic solutions of HCW equations, Shibata and Ichikawa [22] considered formation and reconfiguration problems by feedback control. The main performance index is the L_1-norm of the feedback control, which corresponds to the total velocity change. Numerical simulations with various initial and final conditions show that the L_1-norm of the feedback control designed by the LQR theory decreases monotonically with

L_2-norm, as the penalty on control becomes arbitrarily large. Using this fact, L_1 suboptimal controllers were designed, and applied to the nonlinear relative dynamics. The notion of NCVE was extended by Ichikawa [23] to discrete-time systems and periodic systems. An open-time reconfiguration problem with impulsive maneuvers was studied by Ichimura and Ichikawa [24], and optimal three impulse controls for the HCW system are derived. Noting that the discretized system inherits NCVE [23], l_1 suboptimal impulsive feedback controls were designed and applied to the nonlinear relative dynamics. Shibata and Ichikawa [22] also showed the NCVE property of the TH equations with three independent thrusters, and considered the reconfiguration problem along an eccentric reference orbit using the LQR theory of the periodic system [25].

In [15, 22, 24], designed feedback controls were applied to the original nonlinear relative dynamics. However, periodic relative orbits used for formation are not those of the nonlinear relative dynamics, but those of the HCW equations. To maintain these orbits, control inputs are necessary for all time, even though they might be small. In this paper, periodic orbits of the HCW system are replaced by those of the original nonlinear relative dynamics, and the corresponding formation and reconfiguration problems are considered. Periodic solutions of the nonlinear relative dynamics were used by Gurfil [26] for the initialization problem, where given initial conditions of the nonlinear relative dynamics are adjusted by a single impulse to those of a periodic solution. Using an energy matching condition, the initialization problem with minimum velocity change was solved. However, this method is not applicable to a formation problem with a given relative orbit nor to a reconfiguration problem. The relative motion of the follower with respect to the leader is periodic if and only if the follower is in an inertial orbit with its semimajor axis equal to the radius of the circular reference orbit. Using this fact, initial conditions of the nonlinear dynamics, which yield periodic solutions, are explicitly determined by the initial positions of two satellites in their inertial orbits. First, two inertial orbits are assumed to be coplanar, and the initial positions of two satellites are given in the perifocal reference frame associated with the follower's eccentric orbit. The corresponding initial conditions of the nonlinear relative dynamics are characterized by the initial true anomaly, mean motion, semimajor axis and eccentricity of the follower's inertial orbit. The follower's eccentric orbit is then rotated around one of the axes of the perifocal reference frame in the orbit plane, and in each case, initial conditions of periodic solutions are characterized by the same parameters and the rotation angle. Initial conditions of all non-coplanar relative orbits are generated by the combination of two rotations. Using these periodic solutions of the nonlinear relative dynamics, formation and reconfiguration problems are formulated, and as in [22], L_1 suboptimal feedback controls are designed by the LQR theory. To compare the performances of feedback controls, a reconfiguration problem of Shibata and Ichikawa [22] is modified by replacing the initial conditions of an HCW periodic orbit by those of the periodic orbit of the nonlinear dynamics with the same initial positions. Then L_1- and L_2-norms of the feedback controls and settling times are computed. Two examples of a more general coplanar orbit and a non-coplanar orbit are also given.

The paper is organized as follows. Section 1 is Introduction. Section 2 introduces the equations of the relative motion and their state space form. Section 3 gives the characterization of initial conditions of periodic solutions of the nonlinear relative dynamics, and Section 4 formulates formation and reconfiguration problems. Section 5 discusses the design of feedback controls, and finally Section 6 presents simulation results on three examples.

2 Equations of Relative Motion

Consider two satellites subject to the central gravity field of the Earth, one of which is flying in a given circular orbit of radius R_0 and is referred to as a leader, and the other flying nearby is referred to as a follower. The relative motion of the follower with respect to the leader is given by Newton's equations of motion as follows [4]

$$\begin{aligned}
\ddot{x} &= 2n\dot{y} + n^2(R_0 + x) - \frac{\mu}{R^3}(R_0 + x) + u_x, \\
\ddot{y} &= -2n\dot{x} + n^2 y - \frac{\mu}{R^3} y + u_y, \\
\ddot{z} &= -\frac{\mu}{R^3} z + u_z,
\end{aligned} \tag{1}$$

where the coordinate system (x, y, z) is fixed at the center of mass of the leader, x-, y- and z- axes are along the radial direction, the flight direction of the leader, and the normal direction respectively (see Fig. 1), μ is the gravitational parameter of the Earth, $n = (\mu/R_0^3)^{1/2}$ the orbit rate of the leader, $R = [(R_0+x)^2 + y^2 + z^2]^{1/2}$, and u_x, u_y and u_z are the control accelerations. The linearized equations around the null solution $x = y = z = 0$ are given by

$$\ddot{x} = 2n\dot{y} + 3n^2 x + u_x, \tag{2}$$

$$\ddot{y} = -2n\dot{x} + u_y, \tag{3}$$

$$\ddot{z} = -n^2 z + u_z, \tag{4}$$

which are known as Hill-Clohessy-Wiltshire (HCW) equations. The in-plane motion is determined by Eqs. (2) and (3), and is independent of the out-of-plane motion given by Eq. (4). The solution of HCW equations is periodic if and only if the CW condition $\dot{y}_0 = -2nx_0$ holds. In this case the in-plane motion is given by [22]

$$\begin{aligned}
x(t) &= a\cos(nt + \alpha), \\
y(t) &= d - 2a\sin(nt + \alpha),
\end{aligned} \tag{5}$$

where

$$\begin{aligned}
a &= \left[(3x_0 + 2\dot{y}_0/n)^2 + (\dot{x}_0/n)^2\right]^{1/2}, \quad d = y_0 - 2\dot{x}_0/n, \\
\cos\alpha &= -(1/a)\left(3x_0 + 2\dot{y}_0/n\right), \quad \sin\alpha = -\dot{x}_0/(na).
\end{aligned} \tag{6}$$

It forms an ellipse

$$\frac{x^2}{a^2} + \frac{(y-d)^2}{(2a)^2} = 1. \tag{7}$$

in (x, y) plane, and is useful for formation flying as well as proximity operations such as inspection and repair. Defining

$$\boldsymbol{x} = [x \;\; y \;\; \dot{x} \;\; \dot{y} \;\; z \;\; \dot{z}]^T, \;\; \boldsymbol{u} = [u_x \;\; u_y \;\; u_z]^T,$$

the HCW equations in the state space form become

$$\dot{\boldsymbol{x}} = A\boldsymbol{x} + B\boldsymbol{u}, \tag{8}$$

where

$$A = \begin{bmatrix} 0 & 0 & 1 & 0 & 0 & 0 \\ 0 & 0 & 0 & 1 & 0 & 0 \\ 3n^2 & 0 & 0 & 2n & 0 & 0 \\ 0 & 0 & -2n & 0 & 0 & 0 \\ 0 & 0 & 0 & 0 & 0 & 1 \\ 0 & 0 & 0 & 0 & -n^2 & 0 \end{bmatrix}, \quad B = \begin{bmatrix} 0 & 0 & 0 \\ 0 & 0 & 0 \\ 1 & 0 & 0 \\ 0 & 1 & 0 \\ 0 & 0 & 0 \\ 0 & 0 & 1 \end{bmatrix},$$

and Eq. (1) is rewritten in a semilinear form

$$\dot{\boldsymbol{x}} = A\boldsymbol{x} + B\boldsymbol{u} + Bg(\boldsymbol{x}), \tag{9}$$

where

$$g(\boldsymbol{x}) = [\ -3n^2x - (R_0 + x)(\mu/R^3 - n^2) \quad -y(\mu/R^3 - n^2) \quad -z(\mu z/R^3 - n^2)\ ]^T.$$

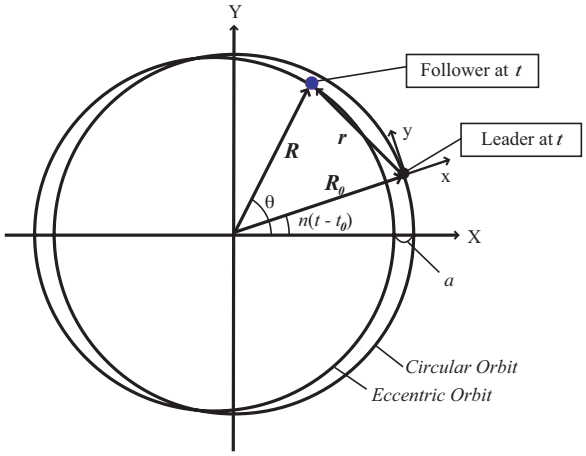

Figure 1: Leader and follower at t: coplanar.

3 Periodic Solutions of Relative Dynamics and Their Initial Conditions

Although periodic solutions of the HCW equations given by Eq. (5) are useful for formation flight and various other operations, they are not free motions of Eq. (1), and hence control efforts are required to maintain them. In this section, initial conditions of periodic solutions of Eq. (1) will be characterized. Assume that the follower is in an eccentric orbit $\Gamma = (A_0, \boldsymbol{e})$ in the inertial frame, where A_0 is the semimajor axis and $\boldsymbol{e}$ the eccentricity vector. Let (X, Y, Z) be its perifocal reference frame whose origin is the center of the earth and the X axis is in the direction of the eccentricity vector $\boldsymbol{e}$. Assume first that two inertial orbits are

coplanar as shown in Fig. 1, where $\boldsymbol{R}$, $\boldsymbol{R_0}$ are the position vectors of the follower and the leader respectively, and $\boldsymbol{r}$ is the relative position vector. If the X coordinate of the perigee is $A_0 - a$, then the eccentricity $e = |\boldsymbol{e}| = a/A_0$. Let t_0 be the time at which the leader is in the direction of $\boldsymbol{e}$ (on the X axis). Let $\theta(t)$ be the true anomaly of the follower, and set $\theta_0 = \theta(t_0)$. Below the initial conditions of Eq. (1) at t_0 will be calculated. Recall that the relative motion of the follower is periodic if and only if $A_0 = R_0$, because in this case periods of the circular and eccentric orbits coincide.

Note that $\boldsymbol{r}(t)$ in the (X, Y, Z) coordinate system is given by

$$\boldsymbol{r}(t) = \boldsymbol{R}(t) - \boldsymbol{R}_0(t) = \begin{bmatrix} R(t)\cos\theta(t) - R_0 \cos n(t-t_0) \\ R(t)\sin\theta(t) - R_0 \sin n(t-t_0) \\ 0 \end{bmatrix}, \tag{10}$$

where $R = |\boldsymbol{R}|$ is given by

$$R(t) = p/(1 + e\cos\theta(t)),\ p = A_0(1-e^2).$$

To find the relative velocity of the follower, the lemma below is useful.

Lemma 3.1.

$$\begin{aligned} p\,\dot{\theta}(t) &= (\mu/p)^{1/2}(1 + e\cos\theta(t))^2, \\ p\,\frac{d}{dt}\cos(\theta(t)+\beta)/(1+e\cos\theta(t)) &= -(\mu/p)^{1/2}(\sin(\theta(t)+\beta) + e\sin\beta), \\ p\,\frac{d}{dt}\sin(\theta(t)+\beta)/(1+e\cos\theta(t)) &= (\mu/p)^{1/2}(\cos(\theta(t)+\beta) + e\cos\beta), \end{aligned}$$

where β is an arbitrary phase angle.

The first equation follows from the Kepler's second law concerning the area velocity, while other two equalities are obtained by direct differentiation.

Note that the angular velocity of the rotating frame (x, y, z) is $\boldsymbol{\omega} = [0\ \ 0\ \ n]^T$ and that the derivatives of $\boldsymbol{r}(t)$ in the (X, Y, Z)- and (x, y, z) frames denoted respectively by $\dot{\boldsymbol{r}}$ ($d\boldsymbol{r}/dt$) and $\delta\boldsymbol{r}/\delta t$ are related by the following equation [4]

$$\dot{\boldsymbol{r}} = \frac{d\boldsymbol{r}}{dt} = \frac{\delta\boldsymbol{r}}{\delta t} + \boldsymbol{\omega}\times\boldsymbol{r}.$$

Hence the relative velocity $\delta\boldsymbol{r}/\delta t$ expressed in the (X, Y, Z) coordinate system is given by

$$\begin{aligned} \frac{\delta\boldsymbol{r}}{\delta t}(t) &= \dot{\boldsymbol{r}} - \boldsymbol{\omega}\times\boldsymbol{r}(t) = \dot{\boldsymbol{R}} - \boldsymbol{\omega}\times\boldsymbol{R}(t) \\ &= \begin{bmatrix} -\frac{n_0 A_0}{\sqrt{1-e^2}}\sin\theta(t) + nR(t)\sin\theta(t) \\ \frac{n_0 A_0}{\sqrt{1-e^2}}(\cos\theta(t) + e) - nR(t)\cos\theta(t) \\ 0 \end{bmatrix}, \end{aligned} \tag{11}$$

where the equality $\delta\boldsymbol{R_0}(t)/\delta t = 0$, Lemma 3.1 with $\beta = 0$, and $(\mu/p)^{1/2} = n_0 A_0/(1-e^2)^{1/2}$, $n_0 = (\mu/A_0^3)^{1/2}$ are used. Thus the relative velocity at t_0 is

$$\frac{\delta\boldsymbol{r}}{\delta t}(t_0) = \begin{bmatrix} -\frac{n_0 A_0}{\sqrt{1-e^2}}\sin\theta_0 + \frac{nA_0(1-e^2)}{1+e\cos\theta_0}\sin\theta_0 \\ \frac{n_0 A_0}{\sqrt{1-e^2}}(\cos\theta_0 + e) - \frac{nA_0(1-e^2)}{1+e\cos\theta_0}\cos\theta_0 \\ 0 \end{bmatrix}. \tag{12}$$

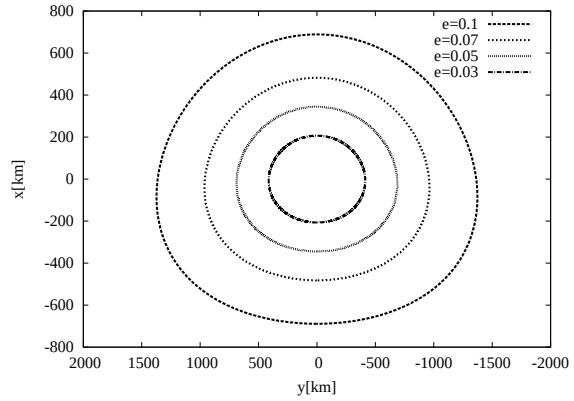

Figure 2: Periodic relative orbits ($\theta_0 = 0$).

Because $\delta \boldsymbol{r}/\delta t$ in two coordinate systems (X, Y, Z) and (x, y, z) coincide at t_0, Eq. (12) is also the relative velocity in the (x, y, z) coordinate system. Hence, Eq. (10) with $t = t_0$ and Eq. (12) give the initial positions and velocities at t_0, i.e.,

$$\begin{bmatrix} x(t_0) \\ y(t_0) \\ z(t_0) \end{bmatrix} = \begin{bmatrix} \frac{A_0(1-e^2)}{1+e\cos\theta_0}\cos\theta_0 - R_0 \\ \frac{A_0(1-e^2)}{1+e\cos\theta_0}\sin\theta_0 \\ 0 \end{bmatrix}, \tag{13}$$

$$\begin{bmatrix} \dot{x}(t_0) \\ \dot{y}(t_0) \\ \dot{z}(t_0) \end{bmatrix} = \begin{bmatrix} -\frac{n_0 A_0}{\sqrt{1-e^2}}\sin\theta_0 + \frac{n_0 A_0(1-e^2)}{1+e\cos\theta_0}\sin\theta_0 \\ \frac{n_0 A_0}{\sqrt{1-e^2}}(\cos\theta_0 + e) - \frac{n_0 A_0(1-e^2)}{1+e\cos\theta_0}\cos\theta_0 \\ 0 \end{bmatrix}. \tag{14}$$

The initial conditions can be directly derived from $\boldsymbol{r}(t)$ in the system (x, y, z) given by

$$\begin{bmatrix} x(t) \\ y(t) \\ z(t) \end{bmatrix} = \begin{bmatrix} R(t)\cos[\theta(t) - n(t-t_0)] - R_0 \\ R(t)\sin[\theta(t) - n(t-t_0)] \\ 0 \end{bmatrix}.$$

In fact $t = t_0$ yields Eq. (13), and the derivative at t_0 gives Eq. (14).

Eqs. (13) and (14) with $A_0 = R_0$ and $n_0 = n$ yield a periodic solution of Eq. (1), and the following theorem holds.

Theorem 3.1. Let $\Gamma = (R_0, \boldsymbol{e})$ be an inertial coplanar eccentric orbit of the follower. Let t_0 be the time at which the leader is in the direction of $\boldsymbol{e}$, and let $\theta_0 = \theta(t_0)$. Then the relative motion of the follower with

respect to the leader is periodic, and the initial conditions of Eq. (1) at t_0 are given by

$$\begin{bmatrix} x(t_0) \\ y(t_0) \\ z(t_0) \end{bmatrix} = \begin{bmatrix} \frac{R_0(1-e^2)}{1+e\cos\theta_0}\cos\theta_0 - R_0 \\ \frac{R_0(1-e^2)}{1+e\cos\theta_0}\sin\theta_0 \\ 0 \end{bmatrix}, \tag{15}$$

$$\begin{bmatrix} \dot{x}(t_0) \\ \dot{y}(t_0) \\ \dot{z}(t_0) \end{bmatrix} = \begin{bmatrix} -\frac{nR_0}{\sqrt{1-e^2}}\sin\theta_0 + \frac{nR_0(1-e^2)}{1+e\cos\theta_0}\sin\theta_0 \\ \frac{nR_0}{\sqrt{1-e^2}}(\cos\theta_0 + e) - \frac{nR_0(1-e^2)}{1+e\cos\theta_0}\cos\theta_0 \\ 0 \end{bmatrix}. \tag{16}$$

Using Eqs. (15) and (16), periodic solutions of Eq. (1) with parameter e are generated in the case $\theta_0 = 0$ and depicted in Fig. 2.

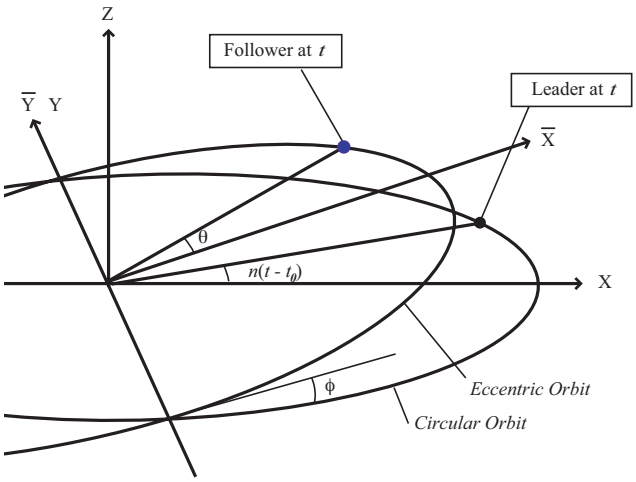

Figure 3: Leader and follower at t: non-coplanar.

Now consider non-coplanar orbits of the follower and their associated initial conditions of Eq. (1). Most practical non-coplanar orbits are generated by rotating coplanar orbits around their X-axis or Y axis. For definiteness, consider the planar orbit $\Gamma = (R_0, \boldsymbol{e})$, and rotate it around the Y axis by an angle ϕ in the negative direction (see Fig. 3). Denote by $(\bar{X}, \bar{Y}, \bar{Z})$ the resulting perifocal reference frame. Then $Y = \bar{Y}$. The position vector of the follower at time t in the $(\bar{X}, \bar{Y}, \bar{Z})$ coordinate system is

$$\boldsymbol{R}(t) = \begin{bmatrix} R(t)\cos\theta(t) \\ R(t)\sin\theta(t) \\ 0 \end{bmatrix},$$

while in the (X, Y, Z) coordinate system

$$\boldsymbol{R}(t) = C_2(\phi)\begin{bmatrix} R(t)\cos\theta(t) \\ R(t)\sin\theta(t) \\ 0 \end{bmatrix} = \begin{bmatrix} R(t)\cos\theta(t)\cos\phi \\ R(t)\sin\theta(t) \\ R(t)\cos\theta(t)\sin\phi \end{bmatrix}, \tag{17}$$

where $C_2(\phi)$ is the rotation matrix

$$C_2(\phi) = \begin{bmatrix} \cos\phi & 0 & -\sin\phi \\ 0 & 1 & 0 \\ \sin\phi & 0 & \cos\phi \end{bmatrix}.$$

Hence the relative position vector $\boldsymbol{r}$ in the (X, Y, Z) coordinate system becomes

$$\boldsymbol{r}(t) = \begin{bmatrix} R(t)\cos\theta(t)\cos\phi - R_0\cos n(t-t_0) \\ R(t)\sin\theta(t) - R_0\sin n(t-t_0) \\ R(t)\cos\theta(t)\sin\phi \end{bmatrix}. \tag{18}$$

The relative velocity expressed in the (X, Y, Z) coordinate system is then

$$\frac{\delta\boldsymbol{r}(t)}{\delta t} = \dot{\boldsymbol{r}} - \boldsymbol{\omega}\times\boldsymbol{r}(t) \tag{19}$$

$$= \begin{bmatrix} -\frac{n_0A_0}{\sqrt{1-e^2}}\sin\theta(t)\cos\phi + nR(t)\sin\theta(t) \\ \frac{n_0A_0}{\sqrt{1-e^2}}(\cos\theta(t)+e) - nR(t)\cos\theta(t)\cos\phi \\ -\frac{n_0A_0}{\sqrt{1-e^2}}\sin\theta(t)\sin\phi \end{bmatrix}. \tag{20}$$

Hence the initial conditions at t_0 are given by

$$\begin{bmatrix} x(t_0) \\ y(t_0) \\ z(t_0) \end{bmatrix} = \begin{bmatrix} \frac{A_0(1-e^2)}{1+e\cos\theta_0}\cos\theta_0\cos\phi - R_0 \\ \frac{A_0(1-e^2)}{1+e\cos\theta_0}\sin\theta_0 \\ \frac{A_0(1-e^2)}{1+e\cos\theta_0}\cos\theta_0\sin\phi \end{bmatrix}, \tag{21}$$

$$\begin{bmatrix} \dot{x}(t_0) \\ \dot{y}(t_0) \\ \dot{z}(t_0) \end{bmatrix} = \begin{bmatrix} -\frac{n_0A_0}{\sqrt{1-e^2}}\sin\theta_0\cos\phi + \frac{nA_0(1-e^2)}{1+e\cos\theta_0}\sin\theta_0 \\ \frac{n_0A_0}{\sqrt{1-e^2}}(\cos\theta_0+e) - \frac{nA_0(1-e^2)}{1+e\cos\theta_0}\cos\theta_0\cos\phi \\ -\frac{n_0A_0}{\sqrt{1-e^2}}\sin\theta_0\sin\phi \end{bmatrix}. \tag{22}$$

Note that Eqs. (21) and (22) are reduced to Eqs. (13) and (14) if $\phi = 0$. Setting $A_0 = R_0$ and $n_0 = n$, initial conditions of a periodic solution of Eq. (1) are obtained.

Theorem 3.2. Let $\Gamma = (R_0, \boldsymbol{e}, \phi)$ be a non-coplanar eccentric orbit of the follower. Let t_0 be the time at which the leader is in the direction of $P\boldsymbol{e}$, and let $\theta_0 = \theta(t_0)$, where P is the projection onto the orbit plane of the leader. Then the relative motion of the follower with respect to the leader is periodic, and the initial conditions of Eq. (1) at t_0 are given by

$$\begin{bmatrix} x(t_0) \\ y(t_0) \\ z(t_0) \end{bmatrix} = \begin{bmatrix} \frac{R_0(1-e^2)}{1+e\cos\theta_0}\cos\theta_0\cos\phi - R_0 \\ \frac{R_0(1-e^2)}{1+e\cos\theta_0}\sin\theta_0 \\ \frac{R_0(1-e^2)}{1+e\cos\theta_0}\cos\theta_0\sin\phi \end{bmatrix}, \tag{23}$$

and

$$\begin{bmatrix} \dot{x}(t_0) \\ \dot{y}(t_0) \\ \dot{z}(t_0) \end{bmatrix} = \begin{bmatrix} -\frac{nR_0}{\sqrt{1-e^2}}\sin\theta_0\cos\phi + \frac{nR_0(1-e^2)}{1+e\cos\theta_0}\sin\theta_0 \\ \frac{nR_0}{\sqrt{1-e^2}}(\cos\theta_0+e) - \frac{nR_0(1-e^2)}{1+e\cos\theta_0}\cos\theta_0\cos\phi \\ -\frac{nR_0}{\sqrt{1-e^2}}\sin\theta_0\sin\phi \end{bmatrix}. \tag{24}$$

Now rotate the coplanar orbit $\Gamma = (R_0, \boldsymbol{e})$ around the X axis by an angle ϕ in the negative direction, and denote by $(\bar{X}, \bar{Y}, \bar{Z})$ the resulting perifocal reference frame. Then in this case $X = \bar{X}$. The relative position vector is given by Eq. (17) with $C_2(\psi)$ replaced by $C_1(\phi)$, where

$$C_1(\psi) = \begin{bmatrix} 1 & 0 & 0 \\ 0 & \cos\psi & \sin\psi \\ 0 & -\sin\psi & \cos\psi \end{bmatrix},$$

and the initial conditions are given as follows:

$$\begin{bmatrix} x(t_0) \\ y(t_0) \\ z(t_0) \end{bmatrix} = \begin{bmatrix} \frac{R_0(1-e^2)}{1+e\cos\theta_0}\cos\theta_0 - R_0 \\ \frac{R_0(1-e^2)}{1+e\cos\theta_0}\sin\theta_0\cos\psi \\ -\frac{R_0(1-e^2)}{1+e\cos\theta_0}\sin\theta_0\sin\psi \end{bmatrix}, \tag{25}$$

and

$$\begin{bmatrix} \dot{x}(t_0) \\ \dot{y}(t_0) \\ \dot{z}(t_0) \end{bmatrix} = \begin{bmatrix} -\frac{nR_0}{\sqrt{1-e^2}}\sin\theta_0 + \frac{nR_0(1-e^2)}{1+e\cos\theta_0}\sin\theta_0\cos\psi \\ \frac{nR_0}{\sqrt{1-e^2}}(\cos\theta_0 + e)\cos\psi - \frac{nR_0(1-e^2)}{1+e\cos\theta_0}\cos\theta_0 \\ -\frac{nR_0}{\sqrt{1-e^2}}(\cos\theta_0 + e)\sin\psi \end{bmatrix}. \tag{26}$$

General non-coplanar orbits of the follower can be generated by two successive rotations $C_2(\phi)$ and $C_1(\psi)$. In fact, let $(\bar{X}, \bar{Y}, \bar{Z})$ and $(\tilde{X}, \tilde{Y}, \tilde{Z})$ be the perifocal reference frames obtained by rotating (X, Y, Z) around the Y-axis by $-\phi$, and then around the $\bar{X}$-axis by $-\psi$ successively i.e., $C_2(\phi) : (\bar{X}, \bar{Y}, \bar{Z}) \to (X, Y, Z)$, $C_1(\psi) : (\tilde{X}, \tilde{Y}, \tilde{Z}) \to (\bar{X}, \bar{Y}, \bar{Z})$. The position vector of the follower at time t in the $(\tilde{X}, \tilde{Y}, \tilde{Z})$ coordinate system is given by

$$\boldsymbol{R}(t) = \begin{bmatrix} R(t)\cos\theta(t) \\ R(t)\sin\theta(t) \\ 0 \end{bmatrix},$$

and in the (X, Y, Z) coordinate system

$$\boldsymbol{R}(t) = C_2(\phi)C_1(\psi)\begin{bmatrix} R(t)\cos\theta(t) \\ R(t)\sin\theta(t) \\ 0 \end{bmatrix}.$$

The relative position vector $\boldsymbol{r}(t)$ and the relative velocity $\delta\boldsymbol{r}(t)/\delta t$ can be calculated in the same way as Eqs. (18) and (20), which in turn give the initial conditions of Eq. (1). Alternatively, let $C(\boldsymbol{q}) : (\tilde{X}, \tilde{Y}, \tilde{Z}) \to (X, Y, Z)$ be the direction cosine matrix parametrized by the quaternions. Then the position vector $\boldsymbol{R}(t)$ in the $(\tilde{X}, \tilde{Y}, \tilde{Z})$ coordinate system is given by the first equality of Eq. (17) with $C_2(\phi)$ replaced by $C(\boldsymbol{q})$, and the relative position vector and the relative velocity can be calculated in a similar way.

4 Formation and Reconfiguration Problems

In this section, formation and reconfiguration problems based on the periodic relative orbits are formulated. First, a characterization of relative orbits is given. Let (X_0, Y_0, Z_0) be an inertial reference frame such

that the (X_0, Y_0) plane coincides with the orbit plane of the leader. Let $\Gamma = (A_0, \boldsymbol{e})$ be a coplanar inertial orbit of the follower. Then the relative orbit is determined by the initial time t_0 and the initial true anomaly θ_0, and hence it will be denoted by $\gamma = (A_0, \boldsymbol{e}, t_0, \theta_0)$. Similarly, the relative orbit corresponding to a non-coplanar inertial orbit is denoted by $\gamma = (A_0, \boldsymbol{e}, t_0, \theta_0, \phi, \psi)$ if the angles of successive rotations of the planar orbit around the Y-axis and the $\bar{X}$-axis are $-\phi$ and $-\psi$ respectively. The formation problem in a general form is described as follows. For a given initial relative orbit $\gamma_0 = (A_0, \boldsymbol{e}, t_0, \theta_0, \phi_0, \psi_0)$ and a final periodic orbit $\gamma_f = (R_0, \boldsymbol{e}_f, t_{f0}, \theta_{f0}, \phi_f, \psi_f)$, find a feedback control strategy such that the solution of (9) starting form the initial orbit tracks γ_f asymptotically. The performance index of the controller is the L_1-norm, which represents the total velocity change, and hence fuel consumption. If, in particular, the initial orbit is periodic, i.e., $\gamma_0 = (R_0, \boldsymbol{e}_0, t_0, \theta_0, \phi_0, \psi_0)$, it is a reconfiguration problem. Note that two orbits γ_0 and γ_f have different initial times, which is inconvenient for control purposes. Below it will be shown how to calculate the relative state of the final orbit at t_0. Recall that the relative dynamics of the follower is given by (9) so that

$$\dot{\boldsymbol{x}} = A\boldsymbol{x} + B\boldsymbol{u} + Bg(\boldsymbol{x}), \quad \boldsymbol{x}(t_0) = \boldsymbol{x}_0,$$

where the initial condition $\boldsymbol{x}_0$ is determined by γ_0. In order to track γ_f, a virtual satellite is introduced, which follows the free motion of (9), i.e.,

$$\dot{\boldsymbol{x}}_f = A\boldsymbol{x}_f + Bg(\boldsymbol{x}_f), \quad \boldsymbol{x}_f(t_{f0}) = \boldsymbol{x}_{f0}, \tag{27}$$

where $\boldsymbol{x}_{f0}$ is determined by γ_f. Without loss of generality, the inequality $t_0 > t_{f0}$ is assumed. For simplicity, consider a planar orbit $\gamma_f = (R_0, \boldsymbol{e}_f, t_{f0}, \theta_{f0})$ (see Fig 4). Then the relative position and velocity of the virtual satellite at t in the perifocal reference frame of the final orbit $\Gamma = (R_0, \boldsymbol{e}_f)$ are given by

$$\boldsymbol{r}_f(t) = \boldsymbol{R}_f(t) - \boldsymbol{R}_0(t) = \begin{bmatrix} R_f(t)\cos(\theta_f(t) - n(t_0 - t_{f0})) - R_0 \cos n(t - t_0) \\ R_f(t)\sin(\theta_f(t) - n(t_0 - t_{f0})) - R_0 \sin n(t - t_0) \\ 0 \end{bmatrix},$$

where

$$R_f(t) = R_0(1 - e_f^2)/(1 + e_f \cos\theta_f(t)).$$

Hence, as in the previous section,

$$\boldsymbol{r}_f(t_0) = \begin{bmatrix} R_f(t_0)\cos(\theta_f(t_0) - n(t_0 - t_{f0})) - R_0 \\ R_f(t_0)\sin(\theta_f(t_0) - n(t_0 - t_{f0})) \\ 0 \end{bmatrix}, \tag{28}$$

and

$$\begin{aligned} \frac{\delta \boldsymbol{r}_f(t_0)}{\delta t} &= \dot{\boldsymbol{r}_f}(t_0) - \boldsymbol{\omega} \times \boldsymbol{r}_f(t_0) \\ &= \begin{bmatrix} -\frac{nR_0}{\sqrt{1-e_f^2}}[\sin(\theta_f(t_0) - n(t_0 - t_{f0})) - e_f \sin n(t_0 - t_{f0})] + nR_f(t_0)\sin(\theta_f(t_0) - n(t_0 - t_{f0})) \\ \frac{nR_0}{\sqrt{1-e_f^2}}[\cos(\theta_f(t_0) - n(t_0 - t_{f0}))] + e_f \cos n(t_0 - t_{f0})] - nR_f(t_0)\cos(\theta_f(t_0) - n(t_0 - t_{f0})) \\ 0 \end{bmatrix}, \end{aligned} \tag{29}$$

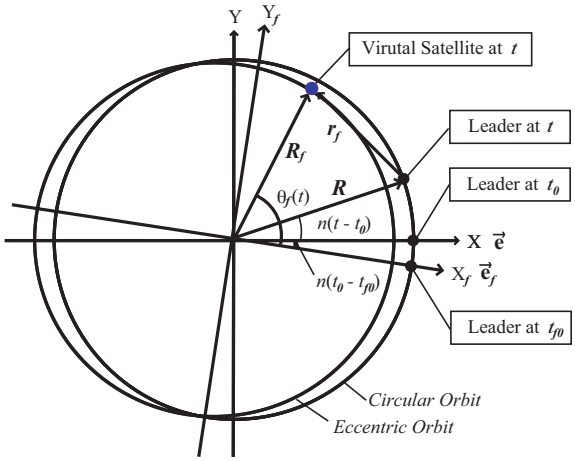

Figure 4: Leader and virtual satellite at t: coplanar.

where Lemma 3.1 with $\beta = n(t_0 - t_{f0})$ is used. The true anomaly $\theta_f(t_0)$ is determined by the Kepler's time equation

$$n(t_0 - t_p) = E_f(t_0) - e_f \sin E_f(t_0)$$

and the following relation

$$\cos\theta_f(t_0) = \frac{\cos E_f(t_0) - e_f}{1 - e_f \cos E_f(t_0)},$$

where E_f is the eccentric anomaly, and the perigee passage time t_p is given by

$$n(t_{f0} - t_p) = E_f(t_{f0}) - e_f \sin E_f(t_{f0}),$$
$$\cos\theta_f(t_{f0}) = \frac{\cos E_f(t_{f0}) - e_f}{1 - e_f \cos E_f(t_{f0})}.$$

The initial condition $\boldsymbol{x}_f(t_0)$ is then obtained by rearranging (28) and (29). When γ_f is non-coplanar, the relative position and velocity at t_0 can be derived using rotational matrices.

In the next section, feedback controls such that $\boldsymbol{x}(t) - \boldsymbol{x}_f(t) \to 0$ as $t \to \infty$ are designed.

5 L_1 Suboptimal Feedback Controllers

To design feedback controllers, the error dynamics

$$\dot{\boldsymbol{\epsilon}} = A\boldsymbol{\epsilon} + B\boldsymbol{u} + B[g(\boldsymbol{x}) - g(\boldsymbol{x}_f)] \tag{30}$$

is introduced, where $\boldsymbol{\epsilon} = \boldsymbol{x} - \boldsymbol{x}_f$. As a main performance index, the L_1-norm of a controller, which represents the fuel consumption, is employed. Recall that the linear part of (30) is the HCW system (8), which is null controllable with vanishing energy (NCVE). This is a property that any state can be steered to the origin with an arbitrary small amount of control energy in the L_2 (square integral) sense, provided that the time duration is free. The system (8) is NCVE if and only if (A, B) is controllable and $X = 0$ is the unique nonnegative solution of the singular algebraic Riccati equation

$$A^T X + XA - XBR^{-1}B^T X = 0, \tag{31}$$

where R is any positive definite matrix. The second condition can be replaced by a more explicit condition: $Re\ \lambda \leq 0$ for every eigenvalue λ of A [21, 23]. The HCW system (8) is NCVE, because it is controllable and the set of eigenvalues of A is $\{0, 0, \pm in, \pm in\}$. Let X be the stabilizing solution of the algebraic Riccati equation

$$A^T X + XA - XBR^{-1}B^T X + Q = 0, \tag{32}$$

where Q is a nonnegative matrix such that $(\sqrt{Q}, A)$ is detectable. Apply the linear feedback control $\boldsymbol{u} = -R^{-1}B^T X\boldsymbol{x}$ to the HCW system (8). Then due to the NCVE property, the L_2-norm of the feedback control decreases to zero as Q decreases to zero (or, equivalently, as R increases to infinity) for any initial condition of Eq. (8). In [22], the reconfiguration problem for the HCW system defined by

$$\begin{aligned} \dot{\boldsymbol{x}} &= A\boldsymbol{x} + B\boldsymbol{u},\ \boldsymbol{x}(0) = \boldsymbol{x}_0^H, \\ \dot{\boldsymbol{x}_f} &= A\boldsymbol{x}_f,\ \boldsymbol{x}_f(0) = \boldsymbol{x}_{f0}^H, \end{aligned} \tag{33}$$

was considered, where $\boldsymbol{x}_0^H$ and $\boldsymbol{x}_{f0}^H$ are the initial conditions of the initial and final orbits of the HCW system. The feedback control

$$\boldsymbol{u} = -R^{-1}B^T X\boldsymbol{\epsilon},\ \boldsymbol{\epsilon} = \boldsymbol{x} - \boldsymbol{x}_f \tag{34}$$

was employed and its L_2- and L_1-norms were computed. It was also applied to Eq. (9) with $\boldsymbol{x}(0) = \boldsymbol{x}_0^H$. In either case, numerical simulations show that the L_2-norm of the feedback converges to zero, and that the L_1-norm decreases monotonically to a positive constant.

In the next section, the feedback controller (34) is employed for the reconfiguration problem of the nonlinear system (30). As performance indices, the L_1- and L_2-norms and the settling time are computed as functions of a parameter of R. Then the performance indices are compared with those of [22]. The feedback controller (34) locally stabilizes Eq. (30), while the feedback controller

$$\boldsymbol{u} = -R^{-1}B^T X\boldsymbol{\epsilon} - [g(\boldsymbol{x}) - g(\boldsymbol{x}_f)] \tag{35}$$

stabilizes globally. Hence, the L_1-norm of the feedback (35) is also calculated for comparison.

6 Simulation Results

For numerical simulations, a circular orbit of the leader of height $h_c = 500$ km is considered. Then the period of this orbit is $T = 5677$ s, and the orbit rate $n = 1.1068\times10^{-3}$ rad/s (see Table 1), where the radius of the Earth R_e and the gravitational constant of the Earth μ are also given. Let $(\boldsymbol{i}, \boldsymbol{j}, \boldsymbol{k})$ be the basis vectors of the inertial frame (X_0, Y_0, Z_0).

Example 6.1. Coplanar formation: synchronized case.
Consider two periodic relative orbits denoted by $\gamma_0 = ((50/R_0)\boldsymbol{i}, 0, 0)$ and $\gamma_f = ((5/R_0)\boldsymbol{i}, 0, 0)$, where $R_0 = R_e + 500$, and consider the reconfiguration from γ_0 to γ_f. In this case, (X_0, Y_0, Z_0) is the perifocal reference system of the two orbits. The X_0 coordinates of the perigee are $R_0 - a$ with $a = 50$, and 5 respectively. Moreover, the leader, follower and virtual satellite are initially on the X_0 axis so that

Table 1: Constants and common parameters

Constants	Values
R_e	6378.136 km
μ	398601 km^3/s^2
Common parameters	**Values**
h_c	500 km
n	1.1068$\times 10^{-3}$ rad/s
T	5677 s

$t_0 = t_{f0} = 0$. Using (15) and (16), the initial conditions of the nonlinear systems (9) and (27) are given respectively by

$$\boldsymbol{x}_0 = [\ -50.0000 \quad 0.00000 \quad 0.00000 \quad 0.11064 \quad 0.00000 \quad 0.00000\ ],$$

$$\boldsymbol{x}_{f0} = [\ -5.00000 \quad 0.00000 \quad 0.00000 \quad 0.01104 \quad 0.00000 \quad 0.00000\ ].$$

Initial conditions of the HCW system (8), which start from the same positions and produce periodic solutions, are given respectively by

$$\boldsymbol{x}_0^H = [\ -50.0000 \quad 0.00000 \quad 0.00000 \quad 0.11044 \quad 0.00000 \quad 0.00000\ ],$$

$$\boldsymbol{x}_{f0}^H = [\ -5.00000 \quad 0.00000 \quad 0.00000 \quad 0.01104 \quad 0.00000 \quad 0.00000\ ].$$

They correspond to the two concentric relative orbits (7) with $d = 0$ km and $a = 50$ km, 5 km, respectively. The initial phases of the follower and the virtual satellite are equal, and $\alpha = \pi$. Note that $\boldsymbol{x}_{f0}$ and $\boldsymbol{x}_{f0}^H$ coincide up to six digits, because these final relative orbits are small and close to each other. This example does not involve the out-of-plane motion, and hence, the four dimensional subsystems of (8) and (9) are used for simulations below. As in [22], Q and R in Eq. (32) are assumed to be diagonal, i.e., $Q = \text{diag}(q_i)$ and $R = 10^r I$ with $q_i = 1.0 \times 10^{-9}$, $i = 1,\ 2$, and $q_i = 0$, $i = 3,\ 4$. The controller (34) with parameter r is applied to the nonlinear system (9) with initial condition $\boldsymbol{x}_0$. The settling time T_s and L_1- and L_2-norms of the feedback controller are depicted in Figs. 5 - 7. As in [22], the settling time is defined as the first time after which inequalities $|x|, |y| < 0.01 r_{min}$ and $|\dot{x}|, |\dot{y}| < 0.01 v_{min}$ are satisfied, where r_{min} is the minimum distance of a point in the final orbit from its center, and v_{min} is the minimum velocity of the follower in the final orbit. The linear case in the figures corresponds to the initial conditions $\boldsymbol{x}_0^H$ and $\boldsymbol{x}_{f0}^H$, while the nonlinear case corresponds to the initial conditions $\boldsymbol{x}_0$ and $\boldsymbol{x}_{f0}$. The HCW case gives the performance indices for the reconfiguration problem of the HCW system (8) and (33). However, L_2- and L_1-norms of the feedback control in three cases are indistinguishable. The L_2-norm decreases to zero as r tends to infinity, confirming the NCVE property, whereas the L_1-norm decreases to a minimum. Minimum values of the L_1-norm are attained at $r = 7$ and are given in Table 2.

Table 2: Minimum L_1-norm

Reference Periodic Orbit	plant	L_1-norm [m/s]
Linear	Nonlinear (Eq. (9))	30.553
Nonlinear	Nonlinear (Eq. (9))	30.776

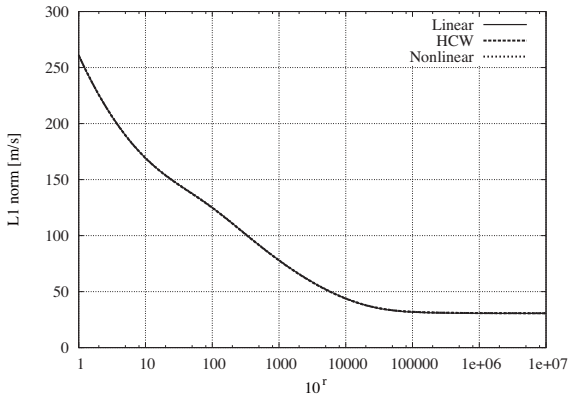

Figure 5: L_1-norm.

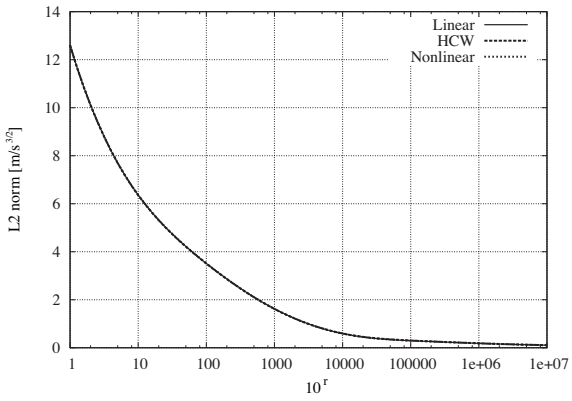

Figure 6: L_2-norm.

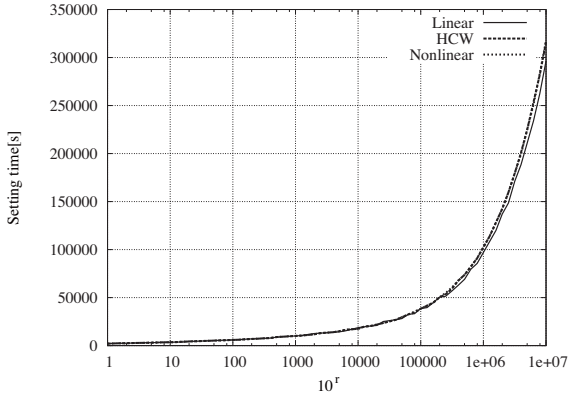

Figure 7: Settling time T_s.

An open-time reconfiguration problem for the HCW system with impulsive maneuvers was solved in [24]. The minimum total velocity change is equal to $n|a_f - a_0|/2$, where a is the size parameter of a periodic orbit given in (7). The minimum is achieved by three impulses along the y-axis. The minimum total velocity change becomes $n|a_f - a_0|$, if impulses are restricted to the x-direction. In this example, $a_f = 50$ km and $a_0 = 5$ km, which yields $n|a_f - a_0|/2 = 24.903$ m/s and $n|a_f - a_0| = 49.806$ m/s. The minimum L_1-norm in Table 2 is larger than the minimum total velocity change by 24%.

For reconfiguration simulations, the parameter is set to $r = 4$, which gives a shorter settling time $T_s = 17527$s. In this case the L_1-norm of the feedback control is 43.917 m/s and the controlled trajectory of the follower is given in Fig. 8. The larger orbit is γ_0, while the smaller one is γ_f. Initial positions of the follower and the virtual satellite are indicated by a dot and a square.

In the reconfiguration problem of the HCW system [22], the nonlinear system (30) is replaced by the HCW system

$$\dot{\boldsymbol{\epsilon}} = A\boldsymbol{\epsilon} + B\boldsymbol{u}. \tag{36}$$

The minimum cost of the LQR problem associated with this is given by $\boldsymbol{\epsilon}_0^T X \boldsymbol{\epsilon}_0$, and further minimization with respect to the initial condition $\boldsymbol{\epsilon}_0$ was performed. When the follower is allowed to stay in the initial orbit and to choose the initial time freely, this determines the best initial position to start control, which minimizes the L_2-norm of the controller. Then the L_1-norm also decreases. In Fig. 9, L_1-norms are plotted against the initial phase $0 \leq \alpha \leq 2\pi$. The best initial position in the nonlinear case is $\alpha = 3.92$, while in other two cases $\alpha = 3.97$. Finally, the nonlinear feedback (35) with $r = 4$ is applied to (9). The L_1-norm is 44.127 m/s and the settling time is $T = 17481$ s. The L_1-norm increases by 0.5%. This simulation indicates that the linear feedback controller is also effective for proximity reconfiguration of the nonlinear system (9) and that no extra control efforts are needed to replace HCW orbits by those of the nonlinear relative dynamics.

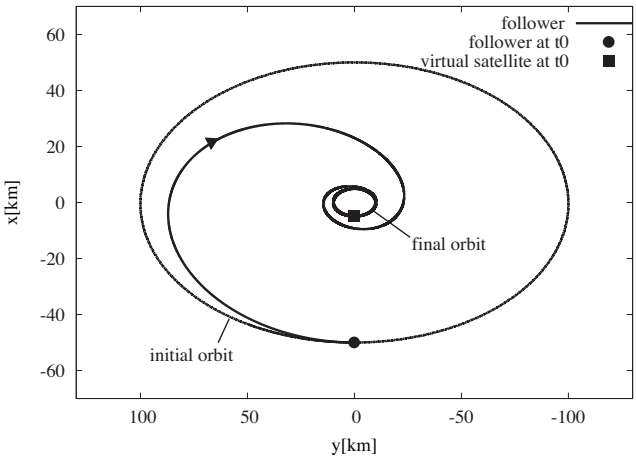

Figure 8: Concentric initial and final orbits and controlled trajectory.

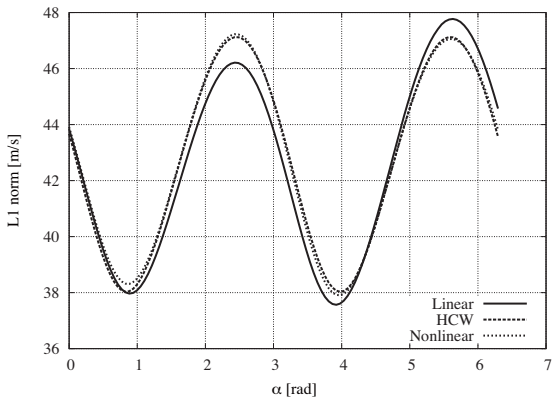

Figure 9: L_1-norm vs initilal phase α.

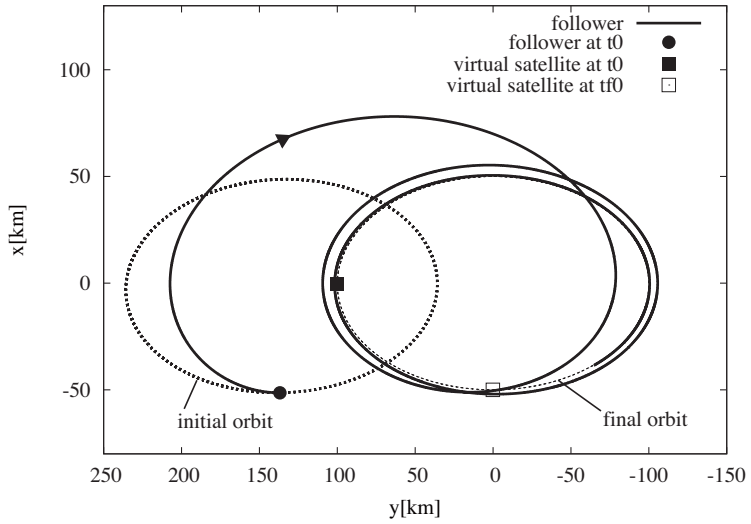

Figure 10: Initial and final orbits and controlled trajectory.

Example 6.2. Coplanar formation: general case.

Consider the initial and final two orbits given by $\gamma = ((50/R_0)\boldsymbol{i}, 0, 0.02)$ and $\gamma_f = ((50/R_0)\boldsymbol{j}, -T/4, 0)$. The angle between $\boldsymbol{e}_0$ and $\boldsymbol{e}_f$ is $\pi/2$. The perifocal reference system of the initial orbit is (X_0, Y_0, Z_0). At time $t_0 = 0$, the leader is on the X_0 axis, i.e., in the direction of $\boldsymbol{e}_0$. At time $t_{f0} = -T/4$, the leader was on the negative part of the Y_0 axis, which is the direction of $\boldsymbol{e}_f$. Hence the perifocal reference system of the final orbit is $(-Y_0, X_0, Z_0)$. Then by (15) and (16), the initial conditions of the follower and the virtual satellite at $t_0 = 0$ and $t_{f0} = -T/4$ are given respectively by

$$\boldsymbol{x}_0 = [\ -51.3577 \quad 136.747 \quad 0.00000 \quad 0.00110 \quad 0.00000 \quad 0.00000\ ],$$

$$\boldsymbol{x}_{f0} = [\ -0.50000 \quad 0.00000 \quad 0.00000 \quad 0.00110 \quad 0.00000 \quad 0.00000\ ].$$

Using (28) and (29), $\boldsymbol{x}_f(0)$ is given by

$$\boldsymbol{x}_f(0) = [\ -0.37611 \quad 99.9983 \quad 0.05522 \quad -0.00017 \quad 0.00000 \quad 0.00000\ ].$$

In this example, the penalty parameters of Example 6.1 are used. In Fig. 10, two orbits γ_0, γ_f and the controlled trajectory are given. The initial position of the follower at $t_0 = 0$ is indicated by a dot and the positions of the virtual satellite at $t_0 = 0$ and $t_{f0} = -T/4$ are shown by squares. The L_1-norm of the feedback control (34) is 115.12 m/s, and the settling time $T_s = 15008$ s. The initial distance $|\boldsymbol{x}_f(0) - \boldsymbol{x}_0| = 62$ and is larger than 45 km of Example 6.1, which leads to the increase of the L_1-norm. The L_1-norm of the nonlinear feedback (35) in this case is 107.91 m/s, and the settling time $T_s = 16424$ s.

Example 6.3. Non-coplanar formation.

Consider the initial and final orbits given respectively by $\gamma_0 = ((50/R_0)\boldsymbol{i}, 0, 0)$ and $\gamma_f = ((5/R_0)\boldsymbol{i}, 0, 0, 0.001)$. The initial orbit is in the orbit plane of the leader (coplanar), and its perifocal reference system is (X_0, Y_0, Z_0). At time $t_0 = 0$, the leader and the follower are on the X_0 axis. The final orbit is the $\phi = 0.001$ [rad] rotation of the coplanar orbit $\gamma_f' = ((5/R_0)\boldsymbol{i}, 0, 0)$, and the initial position of the virtual satellite at $t_{f0} = t_0 = 0$

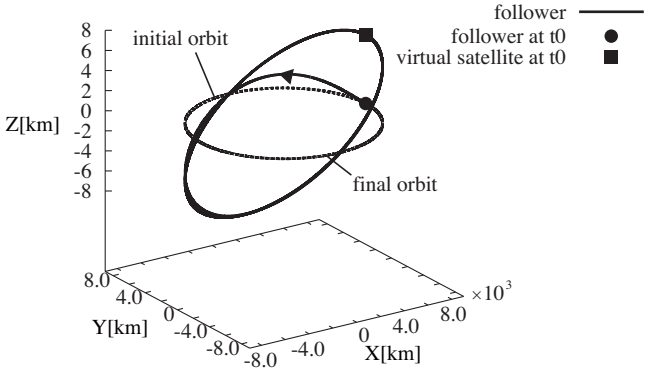

Figure 11: Controlled trajectory in the inertial frame.

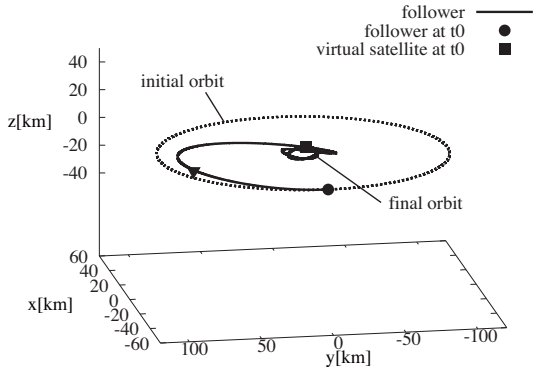

Figure 12: Controlled trajectory in the rotational frame.

is on the $\bar{X}_0$ axis, where $(\bar{X}_0, \bar{Y}_0, \bar{Z}_0)$ is the corresponding perifocal reference system. Then the initial conditions at $t_0 = 0$ of the follower and the virtual satellite are given by

$$\boldsymbol{x}_0 = [\ -50.0000 \quad 0.00000 \quad 0.00000 \quad 0.11064 \quad 0.00000 \quad 0.00000\ ],$$

$$\boldsymbol{x}_{f0} = [\ -5.00344 \quad 0.00000 \quad 0.00000 \quad 0.01105 \quad 6.88280 \quad 0.00000\ ].$$

There are two additional penalty parameters in this example, which are set $q_5 = 1.0 \times 10^{-9}$ and $q_6 = 0$. In Figs. 11 and 12, the initial and final orbits and the controlled trajectory are shown in the inertial frame $(X, Y, Z) = (X_0, Y_0, Z_0)$ and in the rotational frame (x, y, z) respectively. The L_1-norm of the controller is 45.829 m/s and is 4.4% larger than that of Example 6.1, although the sizes of γ_0 and γ_f are the same in two examples. This is due to the fact [24] that the minimum total velocity change for the reconfiguration in the out-of-plane motion is twice larger than that in the in-plane motion. Note that $z_{f0} = 6.88280$. The settling time $T_s = 17527$ s.

7 Conclusions

The conventional formation problem along a circular orbit involves periodic solutions of the Hill-Clohessy-Wiltshire equations. However, a more natural problem is to use periodic solutions of the nonlinear relative dynamics. This paper has given an explicit characterization of the initial conditions of the nonlinear relative dynamics for given initial positions of the leader and the follower in their inertial orbits. When the two inertial orbits are coplanar, the initial conditions are given in terms of the initial true anomaly, mean motion, semimajor axis and eccentricity of the follower orbit. Any non-coplanar orbit of the follower can be generated by two successive rotations of a coplanar orbit around the two axes of the perifocal reference frame. Based on this fact, the initial conditions in the non-coplanar case are derived by multiplying two rotation matrices on those of the coplanar case. When the two inertial orbits have the same size, initial conditions above yield periodic solutions of the nonlinear relative dynamics.

The formation problem in this paper is to find feedback controls which steer the follower asymptotically to a periodic solution of the nonlinear relative dynamics, and the main performance index is the L_1-norm of the control accelerations. The formation problem is solved as the stabilization of the error dynamics, and hence coplanar and non-coplanar formation problems are formulated in a unified manner. The design of feedback controls is based on the null controllability with vanishing energy of the controlled Hill-Clohessy-Wiltshire equations and the linear quadratic regulator theory, which assures the decrease of the L_1-norm as the penalty on control increases. Numerical solutions show that the initial conditions of periodic solutions of the Hill-Clohessy-Wiltshire equations and those of the nonlinear relative dynamics do not differ substantially, if their initial positions are the same. Comparison of the L_1-norms of the feedback controls for the new formation problem and for the conventional problem also shows that the increase in L_1-norm is very little. Thus the introduction of the periodic solutions of the nonlinear relative dynamics to formation problems does not require extra control efforts.

8 Acknowledgments

The authors would like to thank the associate editor and the reviewers for their helpful comments on the paper. The research of the second author was partly supported by the Ministry of Education, Sports, Science and Technology, Japan under Grant-in-Aid for Scientific Research (C), No. 19560785.

References

[1] Clohessy, W. H., and Wiltshire, R. S., “Terminal Guidance System for Satellite Rendezvous,“ Journal of Aerospace Science, Vol. 27, No. 5, 1960, pp. 653-658.

[2] Prussing, J. A., and Conway, B. A., “Orbital Mechanics,” Oxford University Press, New York, 1993, pp. 139-152.

[3] Vallado, D. A., “Fundamentals of Astrodynamics and Applications,” 2nd ed., Microcosm Press, El Segundo, California, and Kluwer Academic Pub, Boston, 2001, pp. 374-399.

[4] Wie, B., “Space Vehicle Dynamics and Control,” AIAA, Reston, Virginia, 1998, pp. 282-285.

[5] Carter, T. E., and Brient, J., “Linearized Impulsive Rendezvous Problem,” *Journal of Optimization Theory and Applications*, Vol. 86, No. 3, 1995, pp. 553-584.
doi: 10.1007/BF02192159

[6] Prussing, J. E., “Optimal Four-Impulse Fixed-Time Rendezvous in the Vicinity of a Circular Orbit,” *AIAA Journal*, Vol. 7, No.5, 1969, pp. 928-935.

[7] Prussing, J. E., “Optimal Two- and Three-Impulse Fixed-Time Rendezvous in the Vicinity of a Circular Orbit,” *AIAA Journal*, Vol. 8, No.7, 1970, pp. 1221-1228.

[8] Carter, T. E., “Optimal Impulsive Space Trajectories Based on Linear Equations,” *Journal of Optimization Theory and Applications*, Vol. 70, No. 2, 1991, pp. 277-297.
doi: 10.1007/BF00940627

[9] Carter, T. E., and Brient, J., “Fuel-Optimal Rendezvous Problem for Linearized Equations of Motion,” *Journal of Guidance, Control, and Dynamics*, Vol. 15, No. 6, 1992, pp. 1411-1416.

[10] Jezewsky, D. J., and Donaldson, J. D., “An Analytic Approach to Optimal Rendezvous Using Clohessy-Wiltshire Equations,” *Journal of the Astronautical Sciences*, Vol. XXVII, No. 3, 1979, pp. 293-310.

[11] Vassar, R. H., and Sherwood, R. B., “Formationkeeping for a Pair of Satellite in a Circular Orbit,” *Journal of Guidance, Control, and Dynamics*, Vol. 8, No. 2, 1985, pp. 235-242.

[12] Leonard, C. L., Hollister, W. M., and Bergmann, E. V., “Orbital Formationkeeping with Differential Drag,” *Journal of Guidance, Control, and Dynamics*, Vol. 12, No. 1, 1989, pp. 108-113.

[13] Redding, D. C., Adams, N., and Kubiak, E. T., “Linear-Quadratic Stationkeeping for the STS Orbiter,” *Journal of Guidance, Control, and Dynamics*, Vol. 12, No. 2, 1989, pp. 248-255.

[14] Kapila, V., Sparks, A. G., Buffington, J. M., and Yan, Q., “Spacecraft Formation Flying: Dynamics and Control,” *Journal of Guidance, Control, and Dynamics*, Vol. 23, No. 3, 2000, pp. 561-564.

[15] Kang, W., Sparks, A., and Banda, S., “Coordinate Control of Multisatellite Systems,” *Journal of Guidance, Control, and Dynamics*, Vol. 24, No. 2, 2001, pp. 360-368.

[16] Campbell, M. E., “Planning Algorithm for Multiple Satellite Clusters,” *Journal of Guidance, Control, and Dynamics*, Vol. 26, No. 5, 2003, pp. 770-780.

[17] Schaub, H., “Relative Orbit Geometry Through Classical Orbit Elemnt Differences,” *Journal of Guidance, Control, and Dynamics*, Vol. 27, No. 5, 2004, pp. 839-848.

[18] Vaddi, S. S., Alfriend, K. T., Vadali, S. R., and Sengupta, P., “Formation Establishment and Reconfiguration Using Impulsive Control,” *Journal of Guidance, Control, and Dynamics*, Vol. 28, No. 2, 2005, pp. 262-268.

[19] Palmer, P., “Optimal Relocatiom of Satellites Flying Near-Circular-Orbit Formations,” *Journal of Guidance, Control, and Dynamics*, Vol. 29, No. 3, 2006, pp. 519-526.

[20] Inalhan, G., Tillerson, M., and How, J. P., “Relative Dynamics and Control of Spacecraft Formations in Eccentric Orbits,” *Journal of Guidance, Control, and Dynamics*, Vol. 25, No. 1, 2002, pp. 48-59.

[21] Priola, E., and Zabczyk, J., “Null Controllability with Vanishing Energy,” *SIAM J. Control Optim.*, Vol. 42, 2003, pp. 1013-1032.
doi: 10.1137/S0363012902409970

[22] Shibata, M., and Ichikawa. A., “Orbital Rendezvous and Flyaround Based on Null Controllability with Vanishing Energy,” *Journal of Guidance, Control, and Dynamics*, Vol. 30, No. 4, July-August, 2007, pp. 934-945.
doi: 10.2514/1.24171

[23] Ichikawa, A., “Null Controllability with Vanishing Energy for Discrete-Time Systems,” *Systems & Control Letters*, Vol. 57, No.1, 2008, pp.34-38.
doi:10.1016/j.sysconle.2007.06.008

[24] Ichimura. Y., and Ichikawa. A., “Optimal Impulsive Relative Orbit Transfer Along a Circular Orbit,” *Journal of Guidance, Control, and Dynamics*, Vol. 31, No. 4, July-August, 2008, pp. 1014-1027.
doi: 10.2514/1.32820

[25] Ichikawa, A., and Katayama, H., “Linear Time-Varying Systems and Sampled-Data Systems,” Springer-Verlag, London, 2001, pp. 19-27.

[26] Gurfil, P., “Relative Motion Between Elliptic Orbits: Generalized Boundedness Conditions and Optimal Formationkeeping,” *Journal of Guidance, Control, and Dynamics*, Vol. 28, No. 4, 2005, pp. 761-767.